Dry gel assisting crystallization of bifunctional CuO-ZnO-Al 2 O 3 /SiO 2 -Al 2 O 3 catalysts for CO 2 Hydrogenation

Zhen Liu, Xiaoqi An, Min Song, Zejia Wang, Yifan Wei, Svetlana Mintova, Girolamo Giordano, Zifeng Yan

Dry gel assisting crystallization of bifunctional $CuO-ZnO-Al_2O_3/SiO_2-Al_2O_3$ catalysts for CO_2 Hydrogenation

Zhen Liu[1,*], Xiaoqi An[1], Min Song[1], Zejia Wang[1], Yifan Wei[1], Svetlana Mintova[1, 2], Girolamo Giordano[3], Zifeng Yan[1,*]

[1] State Key Laboratory of Heavy Oil Processing, College of Chemistry and Chemical Engineering, China University of Petroleum (East China), Qingdao, 266580, China

[2] Normandie Univ, ENSICAEN, UNICAEN, CNRS, Laboratoire Catalyse et Spectrochimie, 6 Boulevard Maréchal Juin, Caen, 14050, France.

[3] Department of Environmental and Chemical Engineering, University of Calabria, Via P. Bucci, 87036 Rende (CS), Italy.

Corresponding Authors: Zhen Liu (zhenliu@upc.edu.cn), Zifeng Yan (zfyancat@upc.edu.cn)

Abstract

A series of bifunctional catalysts $CuO-ZnO-Al_2O_3/SiO_2-Al_2O_3$ (CZA/SA) with different SA/CZA ratios were prepared by dry gel assisting crystallization method. The catalytic performance of bifunctional catalysts for one-step synthesis of methanol (MeOH) and dimethyl ether (DME) from CO_2 hydrogenation was investigated. The results showed that compared with $Cu/ZnO/Al_2O_3$, CZA/SA catalyst significantly improved the selectivity of DME and MeOH and reduced the CO selectivity with moderate CO_2 conversion. The catalyst structure was characterized by X-ray photoelectron spectroscopy (XPS) and temperature-programmed reduction (H_2-TPR), which further confirmed that the active site of methanol generation was the Cu-ZnO interface with a strong interaction rather than solo Cu or ZnO crystallite, which could enhance the hydrogenation function and inhibit reverse water gas shift reaction. Compared with the physical mixing method, the dry gel assisting crystallization method could flexibly adjusted the acid strength and the amounts of acid sites, which was benefit for enhancing dehydration function to improve the selectivity of DME.

Key words

CO_2 hydrogenation, bifunctional catalysts, methanol; dimethyl ether; dry gel

1. Introduction

With the rapid industry development worldwide, CO_2 emission from the combustion of fossil fuels and consumption of chemicals is increasing rapidly. Greenhouse effect and environmental pollution problems were severe in recent years, which have become one of the important global problems urgently needed to be solved[1]. Meanwhile, the growing energy demands requires massive and sustainable energy resources supply, which is becoming crucial because of that most of fossil energy are stored in politically unstable regions. A strategic research area for the development of low-carbon and sustainable production of chemicals and fuels is the utilization of biomass. The use of biomass, especially biowaste from forestry and wood processing, agro-food production and municipal solide waste, to produce renewable energy or chemicals not only provides steady energy resources supply but also aids the sustainable development of human society[2].

However, renewable energy and heat produced from biomass are facing problems related to storage and transport to long distances. High-density energy vectors, such as liquid fuels, are still necessary in all future energy scenario, but they should be derived from alternative resources to fossil fuels. Current technologies for biomass utilization out of combustion (for example, production of bioethanol or biodiesel) are all characterized from two aspects: i) the use of only a fraction of the biomass and ii) the need to use a limited type of resources. There is thus the need to develop a novel technology, which can flexibly use a variety of biowaste to produce chemicals or energy-rich liquid fuels.

Biomass can be converted into CO_2-riched syngas via thermo-chemical processes such as gasification or pyrolysis. Direct production of methanol/dimethylether (DME) from CO_2-riched syngas provide a flexible strategy, which has a wide industrial application prospects for further produce alternative, environmentally-friendly fuels and chemicals usually come from petrochemical industry [3, 4]. Therefore, selective hydrogenation of CO_2 to methanol not only effectively reduces the accumulation of CO_2 and alleviates the greenhouse effect, but also provide alternative route for produce high value-added fuel substitution and chemicals from biomass resources other than petrochemical industry. Despite numerous extensive studies in the past

decades, there is still a lot of controversy about the active site for methanol formation over classic Cu/ZnO based catalyst[5-18]. It was widely believed that Cu, Zn were the active sites for hydrogenation reaction[6, 7]. However, recent studies have shown that perhaps the Cu-ZnO interface is the real active site[8-10, 13, 15], and Cu, Zn can only be considered as the possible precursor of the real active site[8, 12].

However, the one-pass yield of methanol via CO_2 hydrogenation is low because of thermodynamic limitations[19]. In addition, reverse water gas shift reaction easily occurs under the reaction conditions of methanol synthesis[5, 19, 20]. Although researchers found that the use of noble metals or rare earth metal catalysts (such as Pd, Au, Ag, In_2O_3, etc.) instead of conventional CuO-ZnO-Al_2O_3 catalysts can effectively restrain the reverse water gas shift reaction[21-23], the high price of such catalysts limits its large-scale industrial application. The direct synthesis of DME by CO_2 hydrogenation can reduce the thermodynamic limitation of methanol synthesis and restrain the reverse water gas shift (RWGS) reaction. The conversion rate of CO_2 and the selectivity of MeOH and DME are effectively improved. At the same time, it requires only one reactor, reducing the production cost of DME[24, 25].

Dimethyl ether (DME) is known as new green energy in the 21st century because of excellent combustion performance and no pollution[26]. In recent years, DME has attracted a wide spread attention as alternative to liquid petroleum gas (LPG) and diesel[27]. Moreover, DME could be play as an intermediate by methanol dehydration in MTO process, which meets the increasing demand for olefins as a supplementary route to petrochemical industry[28]. At present, the large-scale industrial production of DME is mainly using vapor phase dehydration of methanol. Solid acid materials (such as alumina, molecular sieve) are often used as catalysts with relative mild reaction condition[26].

The catalysts for direct CO_2 to DME conversion should have dual functions that simultaneously catalyze methanol synthesis and dehydration reaction, while reverse water-gas shift reaction should be minimized. Physical mixing method for bifunctional catalyst synthesis is simple, which avoids the interference of two components in the synthesis process. This method can achieve higher CO_2 conversion, but the selectivity of DME is low. Compared with the traditional physical mixing method, the direct formation of metal oxides and acid sites into a homogeneous system at

the microscopic level can make the two components better synergistic effect and achieve relay catalysis[25]. Many strategies for one-pot synthesis of bifunctional catalysts have been implemented, such as impregnation[29], co-precipitation[24, 30, 31], combustion[32], sol-gel method[33] and so on. Due to the close contact between the two components, the reported catalysts prepared by one-pot synthesis strategy had higher CO_2 conversion and DME selectivity (Table S1). However, catalysts also showed relative short lifetime due to relative higher acid strength of zeolite as dehydration component. Yang et al.[34] prepared a core-shell bifunctional catalyst for CO hydrogenation to dimethyl ether by co-precipitation crystallization. On the basis of this, the core-shell structure provided a limited reaction environment, which greatly increased the collision probability between methanol and acid centers and improved the selectivity to dimethyl ether. Ren et al.[30] explored the influence of reaction temperature and reaction pressure on the catalytic performance of bifunctional catalysts. The results show that the optimum reaction temperature is 240 ℃-260 ℃ and the optimum reaction pressure is 2.8 MPa-3.5 MPa.

In this paper, bifunctional CuO-ZnO-Al_2O_3/SiO_2-Al_2O_3 (CZA/SA) catalysts were prepared by dry gel assisting crystallization method. The catalysts were characterized and compared with the catalysts prepared by impregnation-recrystallization method. The active site properties for methanol formation and dehydrogenation were further confirmed by various physical and chemical characterization. At the same time, the optimized ratio of CZA and SA was explored.

2. Experimental

2.1 Catalyst preparation

2.1.1 Preparation of CuO-ZnO-Al_2O_3

CuO-ZnO-Al_2O_3 catalysts with molar ratio of 6/3/1 was prepared by an improved coprecipitation method[30]. The mixed nitrate aqueous solution ($Cu(NO_3)_2$, $Zn(NO_3)_2$ and $Al_2(NO_3)_3$) and Na_2CO_3 aqueous solution were simultaneously added dropwise into a 400 mL three-necked flask with preheated deionized water maintaining at 65 °C-70 °C under violent stirring. During the coprecipitation process, the pH was monitored by a pH meter and maintained at the range of 6.5-7.0 through careful control of dripping speed. At the end of coprecipitation, the pH was adjusted to 7.0 by continue dripping Na_2CO_3 aqueous solution. The obtained suspension was aged in a 70 °C beaker for 60 minutes under violent stirring. The filter cake obtained from

suction filtration was washed with deionized water for at least three times and dried in an oven at 110 ℃ for 12 h. At last, CZA sample was obtained by decomposing metal precipitates, which was calcined in muffle furnace at 360 ℃ for 4 h.

2.1.2 Preparation of CuO-ZnO-Al_2O_3/SiO_2-Al_2O_3 catalyst

Dry gel assisting crystallization method was developed for prepare bifunctional CZA/SA catalysts, among which the solid acid component prepared by traditional synthesis formula of HZSM-5 (0.48TPAOH: 2.0TEOS: 8.0EtOH: 120H_2O: 0.026Al_2O_3). The solution of raw materials was hydrolyzed under stirring at room temperature for 6 hours. The obtained precursor solutions were put into an oven and dried at 110 ℃ for 12 h. The obtained dry gels were physically mixed with certain amount of calcined CZA with different SA/CZA ratio from 1/0.5 to 1/2. A hydrothermal autoclave lining with PTFE was employed for crystallization, in which a certain amount of ethanol aqueous solution was added to the bottom of the lining and a small PTFE open container loaded with abovementioned solid mixture was placed above the lining (Fig. 1). The hydrothermal autoclave was placed in an oven and crystallized at 150 ℃ for 2 days. The obtained samples were washed to neutral and dried in an oven at 110 ℃ for 12 h and calcined in a muffle furnace at 550 ℃ for another 6 h to remove the organic template.

In order to study the superiority, traditional bifunctional catalyst was also prepared by impregnating $CuCl_2$, $ZnCl_2$, $AlCl_3$ with commercial HZSM-5, and the as-prepared sample was recrystallized to recover crystallinity with 0.3 M TPAOH at 150 ℃ for 2 days, then dried overnight at 110 ℃ and calcined in a muffle furnace at 550 ℃ for another 6 h. The resulting sample from impregnation-recrystallization method is denoted as CZA/HZSM-5.

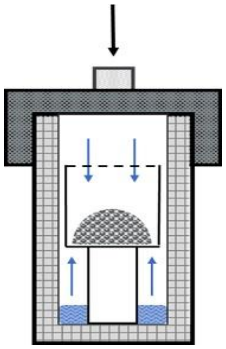

Fig. 1. Improved hydrothermal autoclave for catalysts preparation by dry gel assisting crystallization method

2.2 Catalyst characterization

X-ray diffraction (XRD) was carried out to conduct crystalline structure of the prepared sample on X-ray powder diffractometer X'Pert Pro MPD PXRD produced by PANalytical B.V., using Cu Kα target (λ = 0.15406 nm), tube pressure 40 kV, tube flow 40 mA, scanning range 2θ = 5^o - 50^o.

The reduction properties of CZA after adding SA were analyzed by temperature-programmed reduction (H_2-TPR). The instrument is AutoChem II 2920 Chemisorption Analyzer produced by Micromeritics. 0.1 g (20-40 mesh) sample was put into a U-shaped sample tube. Then the mixture of hydrogen and argon (10% H_2) was pumped. The sample was heated from room temperature to 600 ℃ at a heating rate of 10 ℃/min. Finally, H_2-TPR curve was obtained.

The elemental composition and chemical valence of the samples were analyzed by X-ray photoelectron spectroscopy (XPS) by Thermo Scientific Escalab 250Xi X-ray photoelectron spectroscopy.

The acid properties of the sample were characterized by temperature programmed desorption (NH_3-TPD). The instrument was AutoChem II 2920 Chemisorption Analyzer produced by Micromeritics. Prior to NH_3 adsorption under the mixed atmosphere of NH_3 & He at 70 ℃ for 0.5 h, the sample was pretreated in helium flow at 550 ℃ for 0.5 h. After that, the physically adsorbed NH_3 was removed by purging helium for 0.5 h. Finally, the temperature was raised to the test temperature to obtain the NH_3-TPD curve. The amount of coke deposited on the spent catalyst was measured by TG. The sample was heated to 900 ℃ at a rate of 10 ℃·min^{-1} under 100 mL·min^{-1} flow of air.

The BET surface areas and pore volume of the samples were measured by TriStar 3020 physical adsorption instrument (Micromeritics). The samples were degassed at room temperature for 30 min and then at 300 ℃ for 4 h before the test. The pore structure of the catalysts were determined by measuring the adsorption-desorption data of N_2 at boiling point (77 K).

The morphology and atomic distribution of the catalyst surface were analyzed by SEM-EDS. The SEM analysis was made by Hitachi S-4800 microscope with an acceleration voltage of 0.5-20 kV, fitted with an EDS analyzer.

2.3 Catalytic test

The catalytic evaluation of the catalysts was investigated in a self-designed fixed-bed reactor.

Fig. 2 shows the flow chart of the reactor. 1 g catalyst with particle size of 20-40 mesh (0.425 mm-0.850 mm) was loaded in a stainless reactor tube with 8 mm inner diameter. The catalyst was reduced by H_2/N_2 (1/9, volume ratio) at atmospheric pressure and 280 °C for 4 h with a total flow rate of 100 mL·h^{-1}. After the heating furnace temperature drops to the reaction temperature, slowly increase the pressure to 3.0 MPa to start the reaction The reaction condition was 260 °C, 3.0 MPa, $V(H_2)/V(CO_2)$ = 3.0 and GHSV = 1800 mL·gcat^{-1}·h^{-1}. The products were analyzed online by gas chromatograph Techcomp GC-456C with TCD detector and Porapak-Q (3m*3mm) packed-column.

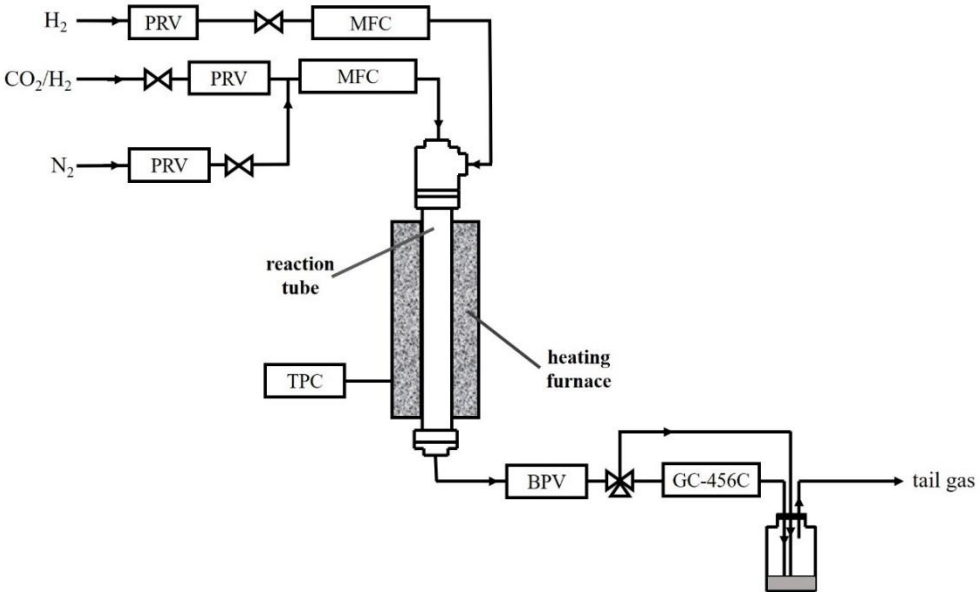

Fig. 2. Flow chart of fixed-bed reactor for CO_2 hydrogenation

PRV: pressure reducing valve, MFC: mass flow controller, BPV: back pressure valve, GC: gas chromatography, TPC: Temperature-programmed controller

The carbon conservation was used to calculate the CO_2 conversion and the selectivity of products such as MeOH and DME. The calculation formula is as follows:

$$X_{CO_2} = \sum_{i=1}^{n} n_i f_i A_i \Big/ \left(\sum_{i=1}^{n} n_i f_i A_i + f_{CO_2} A_{CO_2}\right)$$

$$S_i = n_i f_i A_i \Big/ \sum_{i=1}^{n} n_i f_i A_i$$

where X_{CO2}, i, S_i, n_i, f_i, A_i are CO_2 conversion, different product components, selectivity of product components, C atom number of product components, correction factor of product

components, peak area of product components, respectively.

3. Result and discussion

3.1 Structural property of catalysts

Fig. 3 shows the XRD patterns of CZA, CZA/SA, CZA/HZSM-5 and HZSM-5 samples. It can be seen from Fig. 3a that three diffraction peaks appeared in all samples at 2θ = 30°-40°, which the peaks at 2θ=31.8° and 8.8° are ascribed to the diffraction patterns of ZnO and CuO, respectively[35, 36]. The wide peak at 2θ = 35.5° might be caused by the overlapping of diffraction peaks of ZnO at 2θ = 34.5°, 36.1° and CuO at 2θ = 35.4°[37]. In addition, the classical X-ray diffraction peaks of HZSM-5 also could be observed in the range of 2θ = 7°-9° and 2θ = 22°-25° on CZA/HZSM-5 catalyst synthesized by impregnation-recrystallization method. However, the diffraction peak of HZSM-5 zeolite was not observed in the bifunctional catalyst prepared by dry gel assisting crystallization method, which means that the addition of CZA into system strongly inhibited the crystallization of HZSM-5[38]. It should be mentioned that no corresponding diffraction peak of Al_2O_3 was observed in all catalysts, indicating that Al_2O_3 was present in the catalyst in amorphous phase or implanted into aluminosilicate[31]. Compared with CZA/HZSM-5 catalyst, the diffraction peaks of CuO and ZnO in CZA/SA catalyst became weakened and broadened, which confirmed that the crystalline size of CuO-ZnO was smaller than traditional CZA/HZSM-5 sample[31]. The XRD patterns of a series of bifunctional catalysts with different SA/CZA ratios prepared by dry gel assisting crystallization method are shown in Fig. 3b. No obvious diffraction peaks change on CuO and ZnO was obtained, indicating that CZA could stably existed in the crystallization process from a very wide composition range during dry gel assisting crystallization process. The diffraction peaks of CuO and ZnO showed a gradual increase trend with the increase of CZA content.

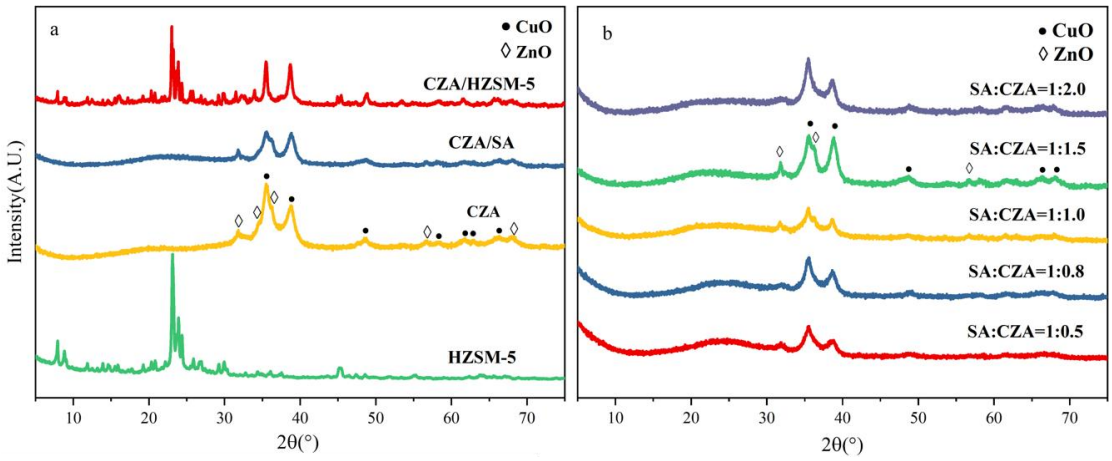

Fig. 3. XRD patterns of the catalysts. (a: CZA, CZA/SA, CZA/HZSM-5 and HZSM-5; b: a series of bifunctional catalysts with different SA/CZA ratios)

The BET Surface areas and the average pore diameter of the catalysts with different SA/CZA ratios are listed in Table 1. From the table, it can be seen that the specific surface area increased from 493 m^2/g to 586 m^2/g when SA/CZA ratio increased from 1/0.5 to 1/0.8, which showed that SA crystallization process was not afftected by introducing small amount of metal oxide. However, sharp decrease on specific surface area was observed when further increasing proportion of CZA, which confirmed that of the porosity of the bifunctional catalyst was mostly contributed by SA component. The pore volume and average pore diameter of the catalyst reached the maximum when SA/CZA=1/1.0. SEM and EDS mapping images of catalyst (SA/CZA =1/1.0) showed that the surface of SA was covered by well dispersed CZA (Fig. S1).

Table 1. Pore structure properties of catalysts with different SA/CZA ratios

Sample	$S_{BET}/(m^2/g)$	$V_t/(cm^3/g)$	$d_{AVG}/(nm)$
SA:CZA=1:0.5	493	0.354	3.0
SA:CZA=1:0.8	586	0.430	3.0
SA:CZA=1:1.0	382	0.559	6.1
SA:CZA=1:1.5	331	0.522	6.0
SA:CZA=1:2.0	198	0.213	4.3

3.2 Reduction of catalysts

The reduction properties of CZA/SA and CZA/HZSM-5 were characterized by H_2-TPR. The reduction curve showed a wide reduction peak (Fig. 4). Given ZnO and Al_2O_3 cannot be reduced during testing temperature range[32, 39, 40], the reduction peak was attributed to the reduction of

CuO species. From the reduction cureve, it is clearly to see that the reduction peaks of the two catalysts were asymmetric, which indicated the overlap peaks resulting from the two reduction processes[41]. There might be two different Cu species with different reducibility in the catalyst, which was consistent to the presumption by Jiang et al[42]. The lower temperature reduction peak was attributed to the reduction of highly dispersed CuO and the higher temperature reduction peak was attributed to the reduction of bulk CuO [43] .

The reduction onset temperature, peak temperature and hydrogen consumption of CZA/SA are higher than those of CZA/HZSM-5 (Table 2). It is interesting to note that compared with the impregnation method, the CZA prepared by dry gel assisting crystallization method had a strong interaction between Cu and ZnO, which increased the reduction temperature of CuO. Meanwhile, the high dispersion of Cu species also caused the result of higher the hydrogen consumption, which was consistent to XRD results.

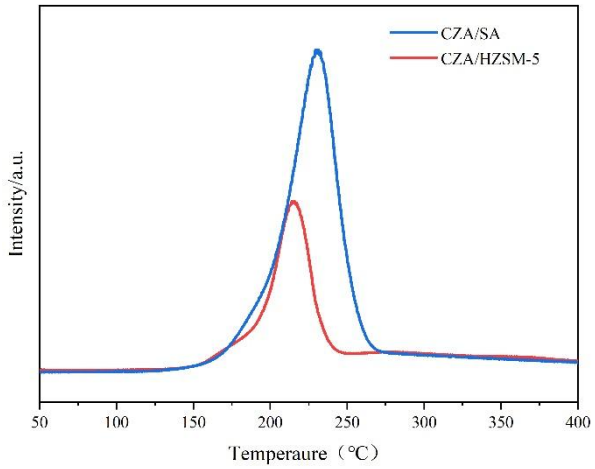

Fig. 4. H_2-TPR profiles of the CZA/SA and CZA/HZSM-5catalysts.

Table 2. The reduction onset temperature, peak temperature and hydrogen consumption of CZA/SA and CZA/HZSM-5

Sample	T_o (℃)	T_M (℃)	H_2 consumption(mmol/g_{cat})
CZA/SA	145.1	231.1	3.86
CZA/HZSM-5	139.0	215.6	2.22

3.3 Chemical state of catalysts

Fig. 5 showed the XPS spectra of bifunctional CZA/SA and CZA/HZSM-5 catalysts. The

peaks at 952.6 eV and 953.5 eV in Fig. 5a and Fig. 5b were attributed to the $Cu2p_{1/2}$ of CZA/HZSM-5 and CZA/SA, respectively, while the peaks at 932.7 eV and 933.7 eV were attributed to the $Cu2p_{3/2}$ of CZA/HZSM-5 and CZA/SA, respectively. The satellite peaks at about 941-942 eV and 961-962 eV indicated that the Cu species in the samples existed in Cu^{2+}[5, 44-46]. Compare with bulk CZA sample with XPS $Cu2p_{3/2}$ peak normally at 932.2 eV attributing to Cu^{2+}[47], the binding energies of $Cu2p_{3/2}$ in CZA/HZSM-5 and CZA/SA were higher than that in CZA. Similar higher binding energy shifts were also observed in the Zn2p spectra in Fig. 5c and Fig. 5d [47]. The peaks of $Zn2p_{3/2}$ in CZA/HZSM-5 and CZA/SA catalysts appeared at 1021.25 eV and 1021.90 eV, respectively, which were higher than that in bulk CZA appeared at 1020.0 eV. The result might be explained that new Cu-Si(Al) and Zn-Si(Al) interfaces with the Cu-O-Si(Al) and Zn−O−Si(Al) bonds in bifunctional catalysts was formed, which resulting in strong interaction with Cu or Zn species. The strong interaction of Cu-Si(Al) and Zn-Si(Al) interfaces makes the lower density of outmost electrons of Cu and Zn, which decreased the shielding effect on X-ray and caused a higher binder energy results. However, the interaction was not as strong as atomically implanted copper phyllosilicate phase with the Si-O-Cu structure, which normally showed characteristic peaks at 935.5 eV in the $Cu2p_{3/2}$ XPS spectrum[38]. It is worth noting that the binding energies of Cu $2p_{3/2}$ and Zn $2p_{3/2}$ in CZA/SA catalysts were higher than those of CZA/HZSM-5 catalysts. It was inferred that the Cu-ZnO-Al_2O_3 catalyst prepared by the Dry gel assisting crystallization method exhibited stronger interaction of Cu-O-Si(Al) and Zn-O-Si(Al) bonds than those in samples prepared by impregnation-recrystallization method. The nearly absence of peak at 935.5 eV to copper phyllosilicate phase demonstrated that dry gel assisting method showed well Cu implant module as Cu-O-Si(Al) interfaces. Combined with XRD results, the smaller crystalline size and better dispersion of Cu species might be resulting in stronger interaction between CuO and ZnO, which might be also led to higher binding energy of Cu and Zn.

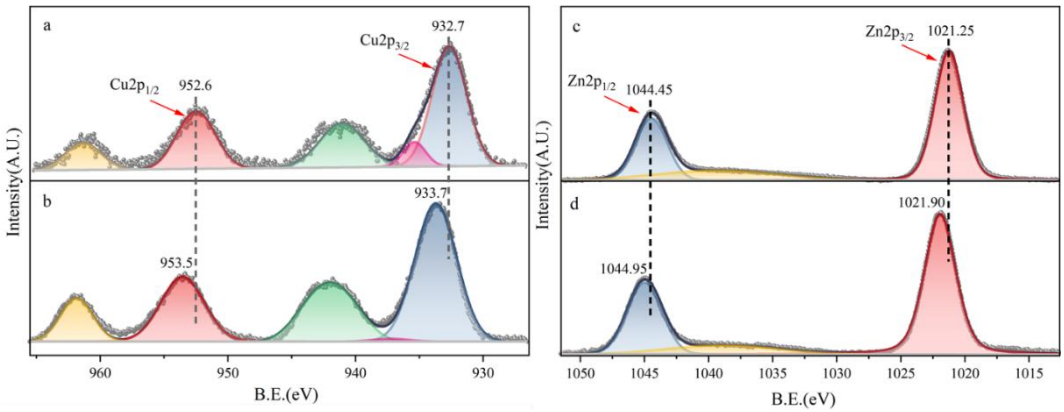

Fig. 5. Cu 2p and Zn 2p XPS spectra of CZA/HZSM-5 (a, c) and CZA/SA (b, d).

3.4 Surface acidity of catalysts

The catalysts with different SA/CZA ratios prepared by dry gel assisting crystallization method were characterized by NH_3-TPD to study the role of acid sites in the synthesis of DME. The desorption curve is shown in Fig. 6 and the peak fitting results are shown in Table 3. It can be observed that each catalyst had three kind of acid site with peak temperatures between 120-130 °C, 200-210 °C and 320-340 °C, respectively, which corresponded to weak acid site, medium strong acid site and strong acid site. Compared with the acid site of HZSM-5 at 150-250 °C, 300-400 °C and 450-550 °C, respectively[48], the three kinds of acid site strength of bifunctional catalyst decreased obviously. The absence of ZSM-5 diffraction peaks in XRD patterns of CZA/SA sample demonstrated that poor crystallization into zeolite led to weaker acid strength. On the other hand, CuO, ZnO and Al_2O_3 might migrated into SiO_2-Al_2O_3 during the crystallization process which would covered some of the acid sites and led to a decrease in acidity[24, 49, 50]. With the increase of CZA content in the bifunctional catalyst, the total acid amount and the number of strong acid sites showed a decreasing trend. It is generally believed that the strong acid site has higher catalytic activity for methanol dehydration to hydrocarbon, while the medium strong acid site favors to form dimethyl ether[51-55]. Therefore, compared with the physical mixing method, the dry gel assisting method could adjust the acid strength and the amounts of acid sites during the preparation of bifunctional catalyst without additional modification of methanol dehydration component to improve the selectivity of DME.

Table 3. The acidity of the CZA/SA catalysts with different SA/CZA ratios

Sample	Acidity (μmol/g_{cat}) NH_3

	Peak 1	Peak 2	Peak 3	Total
SA/CZA=1/0.5	42.36752	137.3683	61.81213	241.548
SA/CZA=1/0.8	32.25195	116.5342	64.80293	213.5891
SA/CZA=1/1.0	35.46852	93.25535	56.49033	185.2142
SA/CZA=1/1.5	35.96557	104.6865	35.73627	176.3883
SA/CZA=1/2.0	14.27406	81.47539	28.68501	124.4469

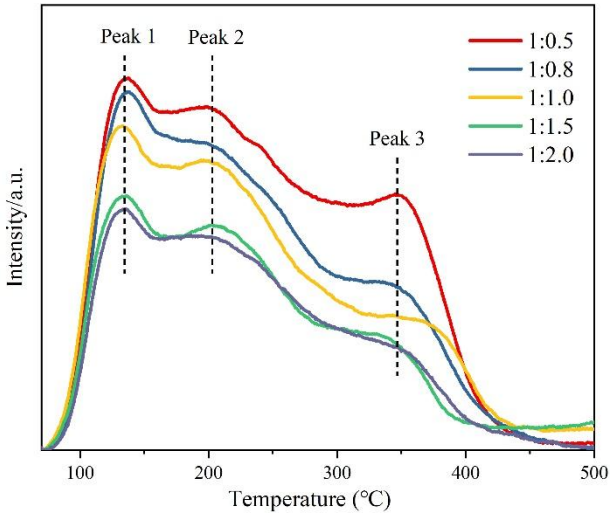

Fig. 6. NH_3-TPD profiles of the catalysts with different SA/CZA ratios from 1/0.5 to 1/2.0

3.5 Catalytic results

The average value of the catalytic test results obtained from the stabilized period of the reaction was taken as the result of CO_2 conversion and product selectivity, which are shown in Table 4. The main by-product of the reaction was CO, in addition to a small number of CH_4. It should be mentioned that no C2+ hydrocarbons were detected over all the catalyst under the reaction condition. Compared with CZA catalyst, the bifunctional catalyst greatly reduced the selectivity of CO by-products after the introduction of acidic component. The selectivity of MeOH and DME increased from 31.50 % to 46.88 % was obtained over CZA/SA catalyst even with weaker acid strength and no distinct ZSM-5 crystallinity. However, CO_2 conversion decreased from 12.47% to 9.36%, which might due to the inhibition of the side reactions of reverse water gas shift. It is interested to notice that CZA/HZSM-5 catalysts prepared by impregnation-recrystallization method showed almost no catalytic activity even both metal

CuO-ZnO component and acid ZSM-5 patterns was observed. As for the CZA/SA catalyst, an improved selectivity to MeOH and DME was obtained over the catalyst even with no distinct ZSM-5, which could be explained by enhancing dehydration function from moderate acid strength and the amounts of acid sites. Moreover, stronger interaction of Cu-O-Si(Al) and Zn-O-Si(Al) or interaction between CuO and ZnO confirmed by XPS might be another reason for the activity enhancement by improving hydrogenation function.

In order to study the optimal SA/CZA ratio of bifunctional catalysts, a series of SA/CZA_x (x = 0.5, 0.8, 1.0, 1.5, 2.0) catalysts were prepared. As shown in Table 4 and Fig. 7, the CO_2 conversion increased from 4.95% to 9.36% when reducing SA addition proportion from 1/0.5 to 1/1.0, which demonstrated that methanol synthesis reaction was the rate controlling step and partially increase the content of CZA component benefited to overall catalyst activity. However, further reducing SA/CZA ratio from 1/1.0 to 1/2.0 led to a slight decrease on CO_2 conversion with significant increase on CO selectivity, which might due to the reason that fewer SA components depressed the subsequent dehydration reaction and strengthen the side RWGS reaction. Different from the physical mixed bifunctional catalyst with the best catalytic performance at SA/CZA = 1/2.0[23]. The catalyst prepared by dry gel assisting crystallization method showed the best performance with SA/CZA ratio of 1/1.0, on which CO_2 conversion and MeOH + DME selectivity were 9.36 % and 46.88 %, respectively. Considering that higher reaction temperature could dynamically accelerate reaction rate, which could benefit for the increase of catalysts activity. However, from the perspective of reaction thermodynamics, increasing reaction temperature is beneficial to RWGS reaction. Here in our case, relative higher selectivities on methanol and DME were obtained, which indicated that SA/CZA with ratio of 1/1.0 could significantly inhibited RWGS reaction at higher reaction temperature of 260 °C. Compared with the hydrothermal method, the dry gel method could fix aluminosilicates precursor into acid component in the water-free micro-region, avoiding the damage of metal components in the harsh hydrothermal crystallization environment to the greatest extent.

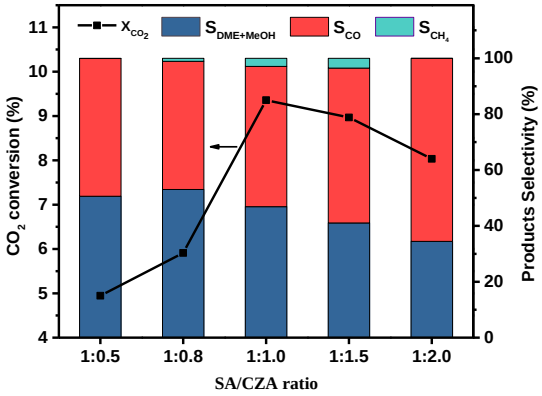

Fig. 7. The CO_2 conversion and product selectivity of the catalysts with different SA/CZA ratios.

Table 4. The CO_2 conversion and product selectivity of different catalysts

Sample	Conversion (%)	Selectivity (%)				
		MeOH	DME	MeOH+DME	CO	CH_4
CZA	12.47%	31.50%	0	31.50%	67.88%	0.62%
HZSM-5/CZA=1/1.0	0.57%	0	0	0	50.75%	49.25%
SA/CZA=1/0.5	4.95%	15.75%	34.88%	50.63%	49.28%	0.09%
SA/CZA=1/0.8	5.91%	17.65%	35.40%	53.05%	45.86%	1.09%
SA/CZA=1/1.0	9.36%	14.28%	32.60%	46.88%	50.20%	2.92%
SA/CZA=1/1.5	8.97%	16.89%	24.17%	41.06%	55.44%	3.50%
SA/CZA=1/2.0	8.03%	11.68%	22.77%	34.45%	65.54%	0.01%

E. Catizzone et al.[25] used Unisim Design R430 software (Honeywell, Morris Stown, NJ, USA) to perform a simulation, which showed that theoretical equilibrium conversion of CO_2 was 23.75% and theoretical equilibrium selectivity of DME, CO and MeOH was 49.5%, 33.5% and 16.4%, respectively. However, the obtained conversion was usually lower than the theoretical equilibrium conversion due to limited contact time between catalysts and reactants, diffusional limitation between hydrogenation and dehydration sites. Additionally, the structure of CZA could be partially undermined to some extent during the crystallization process, which intensified the occurrence of reverse water gas shift (RWGS) reaction and led to lower selectivity to MeOH and DME. The duration test of SA/CZA = 1/1.0 catalyst was tested and shown in Fig. 8, while other

catalysts with different SA/CZA ratio were also tested and presented as Supporting Information Material (Fig. S2 to S4). From the duration data, we can find that the catalytic performance of catalyst reached a stabilized period after 2 hours of reaction time. During the stabilizing period, the CO_2 conversion decreased from 10.73% to 9.26%, while the selectivity of MeOH + DME increased from 39.6% to 47.1% with a synchronous decline on CO selectivity. With the progress of the reaction after reaching stabilized period, the CO_2 conversion rate showed no sign of significant decline with relative stable products selectivity. Previous studies indicated that the Cu-ZnO based CO_2 hydrogenation bifunctional catalyst could be deactivated by the reason of cokes, Cu sintering, and water poisoning[31, 56]. The spent catalyst after reaction was also characterized (Fig. S5 to S6 and Table S2 in Supporting Information Material) to confirm the catalyst stability. XRD patterns of fresh catalyst and spent catalyst revealed that no intensification on the diffraction peak of ZnO or CuO was observed but with some new peaks corresponded to the Cu^0, which means that no obvious sintering or reoxidation was occurred during the reaction. However, BET analysis revealed that a decline on specific surface area was observed, which might due to relative lower stability of SiO_2-Al_2O_3 component. Negligible amount of coke was also determined by TG analysis. All the characterization on spent catalyst revealed that the as-prepared catalysts by dry gel assisting crystallization method showed improved performances on catalyst stability.

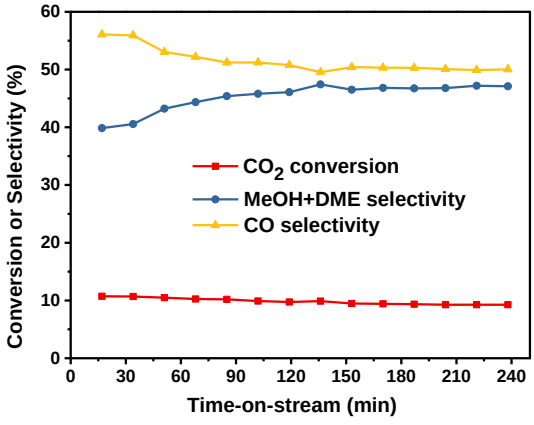

Fig. 8. CO_2 conversion and products selectivity of SA/CZA=1/1.0 catalyst with time on stream.

4. Conclusion

In this paper, CuO-ZnO-Al_2O_3/SiO_2-Al_2O_3 bifunctional catalysts were prepared by dry gel assisting crystallization method for the hydrogenation of CO_2. The products selectivity to

methanol and dimethyl ether was significantly improved from 31.50 % to 46.88 % with a slight decrease on CO_2 conversion over CuO-ZnO-Al_2O_3/SiO_2-Al_2O_3 with weaker acid strength and even no distinct ZSM-5 crystallinity. Compared with the physical mixing method, the acid strength and the amounts of acid sites could be flexibly adjusted during the preparation procedure by dry gel assisting crystallization method, which could significantly improve the selectivity of DME. The characterization of the samples by XPS and H_2-TPR confirmed that the active site of methanol generation was the Cu-ZnO interface, rather than Cu and ZnO. Stronger interaction of Cu-O-Si(Al) and Zn-O-Si(Al) or interaction between CuO and ZnO confirmed by XPS might be another reason for the activity enhancement by improving hydrogenation function. The optimal ratio of CuO-ZnO-Al_2O_3/SiO_2-Al_2O_3 was investigated with SA/CZA ratio of 1/1.0. Duration test and characterization on spent catalyst implied that the catalyst prepared by dry gel assisting crystallization method showed improved performances on catalyst stability.

Acknowledgment

This work was supported by the National Key Technologies R&D Program of China, Key projects of intergovernmental international innovation cooperation (2018YFE0118200), Key Research and Development Plan of Shandong Province (2019JZZY010506), and Key Research and Development Program of Ningxia (2022ZDYF0937).

Reference

[1] J. Artz, T.E. Muller, K. Thenert, J. Kleinekorte, R. Meys, A. Sternberg, A. Bardow, W. Leitner, Sustainable Conversion of Carbon Dioxide: An Integrated Review of Catalysis and Life Cycle Assessment, Chemical Reviews 118(2) (2018) 434-504.

[2] C. Xu, M. Nasrollahzadeh, M. Selva, Z. Issaabadi, R. Luque. Waste-to-wealth: biowaste valorization into valuable bio(nano)materials. Chemical Society Reviews 48(18) (2019) 4791-822.

[3] J.W. Zhong, X.F. Yang, Z.L. Wu, B.L. Liang, Y.Q. Huang, T. Zhang, State of the art and perspectives in heterogeneous catalysis of CO_2 hydrogenation to methanol, Chemical Society Reviews 49(5) (2020) 1385-1413.

[4] L. Grazia, State of art and perspectives about the production of methanol, dimethyl ether and syngas by carbon dioxide hydrogenation, Journal of CO_2 Utilization 27 (2018) 326-354.

[5] S. Kattel, P.J. Ramírez, J.G. Chen, J.A. Rodriguez, P. Liu, Active sites for CO_2 hydrogenation to methanol on Cu/ZnO catalysts, Science 355 (2017) 1296-1299.

[6] S. Kuld, C. Conradsen, P.G. Moses, I. Chorkendorff, J. Sehested, Quantification of zinc atoms in a surface alloy on copper in an industrial-type methanol synthesis catalyst, Angewandte Chemie International Edition 53 (2014) 5941-5945.

[7] S. Kuld, M. Thorhauge, H. Falsig, C.F. Elkjær, S. Helveg, Chorkendorff, J. Sehested, Quantifying the promotion of Cu catalysts by ZnO for methanol synthesis, Science 352(6288) (2016) 969-974.

[8] M. Zabilskiy, V.L. Sushkevich, D. Palagin, M.A. Newton, F. Krumeich, J.A. van Bokhoven, The unique interplay between copper and zinc during catalytic carbon dioxide hydrogenation to methanol, Nature Communications 11(1) (2020) 2409.

[9] S. Kattel, P.J. Ramírez, J.G. Chen, J.A. Rodriguez, P. Liu, Response to Comment on "Active sites for CO_2 hydrogenation to methanol on Cu/ZnO catalysts", Science 357(6354) (2017).

[10] T. Lunkenbein, J. Schumann, M. Behrens, R. Schlogl, M.G. Willinger, Formation of a ZnO overlayer in industrial Cu/ZnO/Al_2O_3 catalysts induced by strong metal-support interactions, Angewandte Chemie International Edition 54(15) (2015) 4544-4548.

[11] O. Martin, C. Mondelli, A. Cervellino, D. Ferri, D. Curulla-Ferre, J. Perez-Ramirez, Operando Synchrotron X-ray Powder Diffraction and Modulated-Excitation Infrared Spectroscopy Elucidate the CO_2 Promotion on a Commercial Methanol Synthesis Catalyst, Angewandte Chemie International Edition 55(37) (2016) 11031-11036.

[12] M. Zabilskiy, V.L. Sushkevich, M.A. Newton, J.A. van Bokhoven, Copper-Zinc Alloy-Free Synthesis of Methanol from Carbon Dioxide over Cu/ZnO/Faujasite, ACS Catalysis 10(23) (2020) 14240-14244.

[13] S.-C. Qi, X.-Y. Liu, R.-R. Zhu, D.-M. Xue, X.-Q. Liu, L.-B. Sun, Causation of catalytic activity of Cu-ZnO for CO_2 hydrogenation to methanol, Chemical Engineering Journal 430 (2022) 132784.

[14] T. Guo, Q. Guo, S. Li, Y. Hu, S. Yun, Y. Qian, Effect of surface basicity over the supported Cu-ZnO catalysts on hydrogenation of CO_2 to methanol, Journal of Catalysis 407 (2022) 312-321.

[15] J. Zhu, D. Ciolca, L. Liu, A. Parastaev, N. Kosinov, E.J.M. Hensen, Flame Synthesis of

Cu/ZnO-CeO_2 Catalysts: Synergistic Metal-Support Interactions Promote CH_3OH Selectivity in CO_2 Hydrogenation, ACS Catalysis 11(8) (2021) 4880-4892.

[16] M. Pori, B. Likozar, M. Marinšek, Z. Crnjak Orel, Preparation of Cu/ZnO-based heterogeneous catalysts by photochemical deposition, their characterisation and application for methanol synthesis from carbon dioxide and hydrogen, Fuel Processing Technology 146 (2016) 39-47.

[17] V.D.B.C. Dasireddy, B. Likozar, The role of copper oxidation state in Cu/ZnO/Al_2O_3 catalysts in CO_2 hydrogenation and methanol productivity, Renewable Energy 140 (2019) 452-460.

[18] M. Pori, I. Arčon, D. Lašič Jurković, M. Marinšek, G. Dražić, B. Likozar, Z. Crnjak Orel, Synthesis of a Cu/ZnO Nanocomposite by Electroless Plating for the Catalytic Conversion of CO_2 to Methanol, Catalysis Letters 149(5) (2019) 1427-1439.

[19] S.S. Dang, H.Y. Yang, P. Gao, H. Wang, X.P. Li, W. Wei, Y.H. Sun, A review of research progress on heterogeneous catalysts for methanol synthesis from carbon dioxide hydrogenation, Catalysis Today 330 (2019) 61-75.

[20] W.J. Cai, Q. Chen, F.G. Wang, Z.C. Li, H. Yu, S.Y. Zhang, L. Cui, C.M. Li, Comparison of the Promoted $CuZnM_xO_y$ (M: Ga, Fe) Catalysts for CO_2 Hydrogenation to Methanol, Catalysis Letters 149(9) (2019) 2508-2518.

[21] K. Chang, T.F. Wang, J.G. Chen, Methanol Synthesis from CO_2 Hydrogenation over CuZnCeTi Mixed Oxide Catalysts, Industrial & Engineering Chemistry Research 58(19) (2019) 7922-7928.

[22] J. Díez-Ramírez, J.A. Díaz, P. Sánchez, F. Dorado, Optimization of the Pd/Cu ratio in Pd-Cu-Zn/SiC catalysts for the CO_2 hydrogenation to methanol at atmospheric pressure, Journal of CO2 Utilization 22 (2017) 71-80.

[23] L.T. Li, C.J. Zhang, X.B. Luo, B. Yang, L.M. Guo, Recent Advances in In_2O_3-based Catalysts for CO_2 Hydrogenation, Materials Reports 35(21) (2021) 21071-21078.

[24] F. Frusteri, M. Cordaro, C. Cannilla, G. Bonura, Multifunctionality of Cu-ZnO-ZrO_2/H-ZSM5 catalysts for the one-step CO_2-to-DME hydrogenation reaction, Applied Catalysis B: Environmental 162 (2015) 57-65.

[25] E. Catizzone, G. Bonura, M. Migliori, F. Frusteri, G. Giordano, CO_2 Recycling to Dimethyl

Ether: State-of-the-Art and Perspectives, Molecules 23(1) (2017).

[26] L.K. Xu, Study of Catalyst for the Dehydration of Methanol to Dimethyl Ether, North University of China, 2016.

[27] X.Y. Yang, S. Sun, J.J. Ding, Y. Zhang, M.M. Zhang, C. Gao, J. Bao, Preparation, Structure and Performance of [CuO-ZnO-Al_2O_3]/[HZSM-5] Core-Shell Bifunctional Catalysts for One-Step Synthesis of Dimethyl Ether from CO_2+H_2, Acta Physico-Chimica Sinica 28(08) (2012) 1957-1963.

[28] P. Pérez-Uriarte, A. Ateka, A.T. Aguayo, A.G. Gayubo, J. Bilbao, Kinetic model for the reaction of DME to olefins over a HZSM-5 zeolite catalyst, Chemical Engineering Journal 302 (2016) 801-810.

[29] R.P. Ye, J. Ding, W. Gong, M.D. Argyle, Q. Zhong, Y. Wang, C.K. Russell, Z. Xu, A.G. Russell, Q. Li, M. Fan, Y.G. Yao, CO_2 hydrogenation to high-value products via heterogeneous catalysis, Nature Communications 10(1) (2019).

[30] S.J. Ren, W.R. Shoemaker, X.F. Wang, Z.Y. Shang, N. Klinghoffer, S.G. Li, M. Yu, X.Q. He, T.A. White, X.H. Liang, Highly active and selective Cu-ZnO based catalyst for methanol and dimethyl ether synthesis via CO_2 hydrogenation, Fuel 239 (2019) 1125-1133.

[31] Y.B. Hu, Y.J. Zhang, J. Du, C.Y. Li, K.J. Wang, L.D. Liu, X.R. Yu, K. Wang, N. Liu, The influence of composition on the functionality of hybrid CuO-ZnO-Al_2O_3/HZSM-5 for the synthesis of DME from CO_2 hydrogenation, RSC Advances 8(53) (2018) 30387-30395.

[32] Y.Y. Zhang, D.B. Li, S.J. Zhang, K.J. Wang, J. Wu, CO_2 hydrogenation to dimethyl ether over CuO-ZnO-Al_2O_3/HZSM-5 prepared by combustion route, RSC Advances 4(32) (2014) 16391-16396.

[33] J.W. Bae, S.H. Kang, Y.J. Lee, K.W. Jun, Effect of precipitants during the preparation of Cu-ZnO-Al_2O_3/Zr-ferrierite catalyst on the DME synthesis from syngas, Journal of Industrial and Engineering Chemistry 15(4) (2009) 566-572.

[34] G. Yang, N. Tsubaki, J. Shamoto, Y. Yoneyama, Y. Zhang, Confinement Effect and Synergistic Function of H-ZSM-5/Cu-ZnO-Al_2O_3 Capsule Catalyst for One-Step Controlled Synthesis, Journal of the American Chemical Society 132(23) (2010) 8129-8136.

[35] L.Y. Li, D.S. Mao, J. Xiao, L. Li, X.M. Guo, J. Yu, Facile preparation of highly efficient

CuO-ZnO-ZrO_2/HZSM-5 bifunctional catalyst for one-step CO_2 hydrogenation to dimethyl ether: Influence of calcination temperature, Chemical Engineering Research and Design 111 (2016) 100-108.

[36] S.H. Xiong, Y. Lian, H. Xie, B. Liu, Hydrogenation of CO_2 to methanol over Cu/ZnCr catalyst, Fuel 256 (2019) 115975.

[37] C. Jeong, J. Kim, J.H. Kim, S. Lee, J.W. Bae, Y.W. Suh, Direct Conversion of CO_2 into Dimethyl Ether over Al_2O_3/Cu/ZnO Catalysts Prepared by Sequential Precipitation, Catalysts 9(6) (2019) 524.

[38] X.J. Cui, W.J. Yan, H.H. Yang, Y. Shi, Y.F. Xue, H. Zhang, Y.L. Niu, W.B. Fan, T.S. Deng, Preserving the Active Cu-ZnO Interface for Selective Hydrogenation of CO_2 to Dimethyl Ether and Methanol, ACS Sustainable Chemistry & Engineering 9(7) (2021) 2661-2672.

[39] N.F.P. Ribeiro, M.M.V.M. Souza, M. Schmal, Combustion synthesis of copper catalysts for selective CO oxidation, Journal of Power Sources 179(1) (2008) 329-334.

[40] C. Baltes, S. Vukojevic, F. Schuth, Correlations between synthesis, precursor, and catalyst structure and activity of a large set of CuO/ZnO/Al_2O_3 catalysts for methanol synthesis, Journal of Catalysis 258(2) (2008) 334-344.

[41] R.D. Purohit, B.P. Sharma, K.T. Pillai, A.K. Tyagi, Ultrafine ceria powders via glycine-nitrate combustion, Materials Research Bulletin 36 (2001) 2711–2721.

[42] J. Xiaoyuan, L. Guanglie, Z. Renxian, M. Jianxin, C. Yu, Z. Xiaoming, Studies of pore structure, temperature-programmed reduction performance, and micro-structure of CuO/CeO_2 catalysts, Applied Surface Science 173 (2001) 208-220.

[43] M. Rhodes, A. Bell, The effects of zirconia morphology on methanol synthesis from CO and H_2 over Cu/ZrO_2 catalystsPart I. Steady-state studies, Journal of Catalysis 233(1) (2005) 198-209.

[44] F. Márquez, A.E. Palomares, F. Rey, A. Corma, Characterisation of the active copper species for the NO_x removal on Cu/Mg/Al mixed oxides derived from hydrotalcites: an in situ XPS/XAES study, Journal of Materials Chemistry 11(6) (2001) 1675-1680.

[45] L.F. Chen, P.J. Guo, M.H. Qiao, S.R. Yan, H.X. Li, W. Shen, H.L. Xu, K.N. Fan, Cu/SiO_2 catalysts prepared by the ammonia-evaporation method: Texture, structure, and catalytic performance in hydrogenation of dimethyl oxalate to ethylene glycol, Journal of Catalysis 257(1)

517 (2008) 172-180.
518 [46] R.T. Figueiredo, M.S. Santos, H.M.C. Andrade, J.L.G. Fierro, Effect of alkali cations on the
519 $CuZnOAl_2O_3$ low temperature water gas-shift catalyst, Catalysis Today 172(1) (2011) 166-170.
520 [47] M. Vijayaraj, C. Gopinath, On the "Active spacer and stabilizer" role of Zn in $Cu_{1-x}Zn_xFe_2O_4$
521 in the selective mono-N-methylation of aniline: XPS and catalysis study, Journal of Catalysis
522 241(1) (2006) 83-95.
523 [48] V. Vishwanathan, K.-W. Jun, J.-W. Kim, H.-S. Roh, Vapour phase dehydration of crude
524 methanol to dimethyl ether over Na-modified H-ZSM-5 catalysts, Applied Catalysis A: General
525 276(1-2) (2004) 251-255.
526 [49] A. García-Trenco, A. Vidal-Moya, A. Martínez, Study of the interaction between components
527 in hybrid CuZnAl/HZSM-5 catalysts and its impact in the syngas-to-DME reaction, Catalysis
528 Today 179(1) (2012) 43-51.
529 [50] J.H. Flores, M.I. Pais da Silva, Acid properties of the hybrid catalyst CuO-ZnO or
530 $CuO-ZnO-Al_2O_3$/H-ferrierite: An infrared study, Colloids and Surfaces A: Physicochemical and
531 Engineering Aspects 322(1-3) (2008) 113-123.
532 [51] S.D. Kim, S.C. Baek, Y.J. Lee, K.W. Jun, M.J. Kim, I.S. Yoo, Effect of γ-alumina content on
533 catalytic performance of modified ZSM-5 for dehydration of crude methanol to dimethyl ether,
534 Applied Catalysis A: General 309(1) (2006) 139-143.
535 [52] S. Hassanpour, F. Yaripour, M. Taghizadeh, Performance of modified H-ZSM-5 zeolite for
536 dehydration of methanol to dimethyl ether, Fuel Processing Technology 91(10) (2010) 1212-1221.
537 [53] N. Khandan, M. Kazemeini, M. Aghaziarati, Dehydration of Methanol to Dimethyl Ether
538 Employing Modified H-ZSM-5 Catalysts, Iranian Journal of Chemical Engineering 6(1) (2009)
539 3-11.
540 [54] S. Hassanpour, M. Taghizadeh, Preparation, Characterization, and Activity Evaluation of
541 H-ZSM-5 Catalysts in Vapor-Phase Methanol Dehydration to Dimethyl Ether, Industrial &
542 Engineering Chemistry Research 49(9) (2010) 4063–4069.
543 [55] G. Bonura, M. Migliori, L. Frusteri, C. Cannilla, E. Catizzone, G. Giordano, F. Frusteri,
544 Acidity control of zeolite functionality on activity and stability of hybrid catalysts during DME
545 production via CO_2 hydrogenation, Journal of CO_2 Utilization 24 (2018) 398-406.

[56] K. Krim, A. Sachse, A. Le Valant, Y. Pouilloux, S. Hocine, One Step Dimethyl Ether (DME) Synthesis from CO_2 Hydrogenation over Hybrid Catalysts Containing Cu/ZnO/Al_2O_3 and Nano-Sized Hollow ZSM-5 Zeolites, Catalysis Letters (2022) https://doi.org/10.1007/s10562-022-03949-w.